Picture Quality Prediction in Image Processing

Vincent Savaux[1], Geoffroy Cormier[2,3], Guy Carrault[3], Moïse Djoko-Kouam[2], Jean-Marc Laferté[2], Yves Louët[1], and Alexandre Skrzypczak[4]

[1] IETR-Supélec, Avenue de la Boulaie, CS 47601, 35576 Cesson-Sévigné, France
[2] ECAM Rennes-Louis de Broglie, CS 29128, 35091 Rennes Cedex 9, France
[3] LTSI, Université de Rennes 1, 35000 Rennes, France
[4] Zodiac Data Systems, 2 rue de Caen, 14740 Bretteville l'Orgueilleuse, France
{vincent.savaux,yves.louet}@supelec.fr,
{geoffroy.cormier,moise.djoko-kouam,jean-marc.laferte}@ecam-rennes.fr,
Alexandre.Skrzypczak@zodiacaerospace.com

Abstract. Interpolations are among the most important tools for image processing. However, whether they are used for image compression and reconstruction purposes or for the increase of the image resolution along vertical, horizontal or both dimensions, the induced interpolation errors are often only qualitatively and a posteriori described. In this paper, we propose to extend a method used in an OFDM context to achieve a quantitative a priori estimation of interpolation errors. As shown by simulations, this estimation proves to be consistent with a posteriori error and quality measurements, such as mean square error (MSE) and peak signal-to-noise ratio (PSNR).

Keywords: Interpolation, a priori estimation, MSE, PSNR.

1 Introduction

Interpolations are often used in image processing when it comes to apply compression and decompression techniques, to achieve reconstruction of damaged images, or resolution change. Although techniques are more and more precise, such an operation inevitably reduces the picture quality, with respect to the original image. The tools allowing the measurement of picture quality are widely described in [1] either by a qualitative and subjective human observation or by quantitative a posteriori measurements. This article deals with a priori picture quality prediction by means of quantitative measurements.

The author of [2] proposed a technique to address the problem of transmitting and archiving large image data, namely in distributed environments. The aim is to achieve high compression ratios while limiting degradations resulting from excessive information loss, using multi-resolution wavelet analysis [3]. No theoretical assumptions or error estimations are given whatsoever, whether predicted or a posteriori calculated. In [4], a detailed state of the art of interpolation techniques used in image processing is presented. Among them, the most commonly used are based on low order polynomial functions, such as the nearest-neighbor (NN), the linear or the cubic interpolations.

A. Elmoataz et al. (Eds.): ICISP 2014, LNCS 8509, pp. 358–366, 2014.

Even in recently published papers, a subjective evaluation by an observer is a common way to compare the performance of different interpolation techniques [5]. A more objective manner is to use picture quality measurements such as the minimum mean square error (MSE) or the peak signal to noise ratio (PSNR), used in [6] to compare different zooming methods. Although these approaches are different, both evaluations prove efficient for the choice of a given interpolation technique, as shown in [7] where objective measurements corroborate human observations. However, these evaluations only provide an a posteriori estimation of interpolation error.

In this paper, we propose a statistics-based method for measuring interpolated picture quality, whose principle has been proposed for the estimation of Rayleigh channels in an orthogonal frequency division multiplexing (OFDM) modulation context [8]. Considering images that can be defined by a sum of random Gaussian processes we analytically determine the picture quality given the chosen interpolation method, the increasing resolution rate and the statistical parameters of the images. Due to their simplicity, the nearest-neighbor and linear interpolations are used to achieve the theoretical developments, but higher order interpolations, such as the bicubic interpolator, shall be investigated in future developments. The main advantage of the proposed method lies in the opportunity to a priori choose the interpolation method, given the targeted image quality. In the following, synthetic images of stars and waves are simulated, but one can easily imagine an application of the proposed method on whole or parts of real pictures.

The rest of this article is organized as follows: Section 2 describes the chosen image model, the interpolations and picture quality measurements used afterward. In Section 3 are developed the statistical analysis from which we obtain the a priori error, and simulations in Section 4 validate the theoretical results. Finally, we draw conclusions and perspectives in Section 5.

2 Images Model

In this section, we present the notations that will be used throughout this paper, as well as the image model and the considered interpolation techniques.

Let S denote a set of N test images, and $I_k \in S$, $k \leq N$ the k^{th} image of the set. Each image of a single set has the same vertical and horizontal resolutions V_{Res} and H_{Res}, and we write out $p_k\,(i,\, j)$ the pixel on the i^{th}row and j^{th}column of image I_k, $0 \leq i \leq V_{Res}$, $0 \leq j \leq H_{Res}$. Keep in mind that, according to the context, $p_k\,(i,\, j)$ could represent either the pixel itself or the value (e. g. the intensity) of the very same pixel.

To comply with the theoretical assumptions made in [8], images within sets must follow a Gaussian distribution. To achieve this, we consider that each image set S is a time series of images whose pixel intensities vary according to coefficients following a Gaussian distribution, i.e.:

$$p_k(i,\, j) = \sum_{m=0}^{M-1} \alpha_{m,k} f_m(i,\, j)\,, \tag{1}$$

with $\alpha_{m,k}$ a zero-mean Gaussian process with variance $\sigma^2_{\alpha_m}$ and f_m a deterministic function that is $\mathcal{C}^2$ on $\mathbb{R}^2$. Then, any image I_k picked from S fulfills the requirements established by [8] to achieve a priori interpolation error estimation. Bearing in mind that we aim at using our technique for any image, as will be discussed in subsequent sections, the way we construct our images is chosen so as to obtain synthetic images which nonetheless resemble real images, such as dark sky dotted with stars, interference patterns or sea clutter. In this paper, we shall present the results obtained for two models:

- the *stars*: the functions f_m in (1) are defined by

$$f^s_m(i,\, j) = e^{-((i-i_m)^2+(j-j_m)^2)/a_m}\,,$$

  where, for $m = 0, .., M-1$, a_m is a fixed real positive coefficient that characterizes the "width" of each function f^s_m, and the couple (i_m, j_m) defines the position of the m^{th} stars on the picture, as depicted in Fig. 1 (a). We also show in the video `https://www.youtube.com/watch?v=ktjHhrs1QKg` a set S composed of $N = 560$ images depicting $M = 18$ stars. The random fluctuations of the star light intensities may simulate the atmospheric disturbances, e.g. the index change or cloudy spells.
- the *waves*: the functions f_m in (1) are defined by

$$f^w_m(i,\, j) = A\cos(2\pi c_{mx} i + 2\pi c_{my} j)\,,$$

  where A, c_{mx} and c_{my} are fixed real coefficients, as depicted in Fig. 1 (b). We also show in the video `https://www.youtube.com/watch?v=XLnq2DHnYC4` a set S composed of $N = 420$ images simulating natural sea waves as a sum of $M = 10$ stationary waves. For a better observation of the waves, a 3D visualization is proposed.

In both models, the varying random coefficients $\alpha_{m,k}$ are simulated by means of a Monte-Carlo method. Given an image I_k picked from a set S built as presented above, we study the effects of interpolations on I_k for scenarios such as subsampling of I_k (for compression purposes, for instance) followed by an interpolation step to get back an image $\hat{I_k}$ similar to I_k, zooming in I_k or stretching I_k along either one or both dimensions.

For the sake of simplicity, we limited ourselves to Nearest-Neighbor and Linear interpolations, performed along one dimension (vertical or horizontal), though we shall study other techniques and two-dimensions interpolations in further works. The results of our a priori interpolation error measurements, which we might call scores, are then compared to the values one obtains a posteriori with mean square error (MSE) and peak signal to noise ratio (PSNR) measurements.

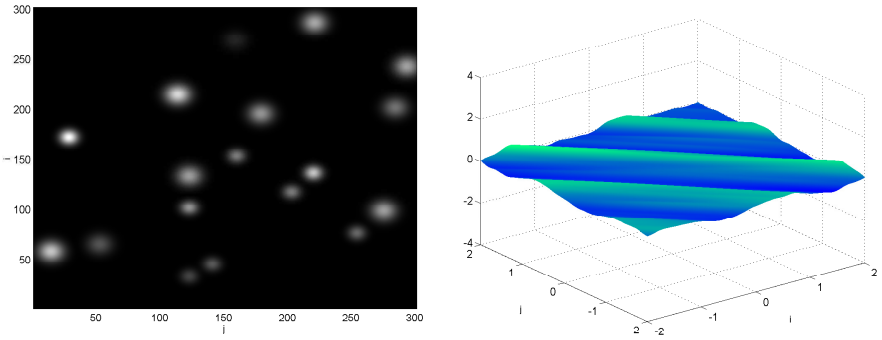

(a) Stars. (b) Waves.

Fig. 1. Two pictures I_k with Gaussian intensities

3 Picture Quality Prediction

According to the previous model, we may reduce the resolution of our images by suppressing either rows or columns. Let us then define S^l the set of N test images obtained after having removed columns from the images of S, and $I_k^l \in S^l$, $k \leq N$ the k^{th} image of the new set. We suppose that the suppressed columns are regularly spaced, with a factor $c = H_{Res}^l / H_{Res}$, where H_{Res}^l is the horizontal resolution of the images I_k^l. Fig. 2 illustrates this with an image taken from the *stars* set, the resolution decreasing from (a) to (b) with $c = H_{Res}^l / H_{Res} = 1/8$.

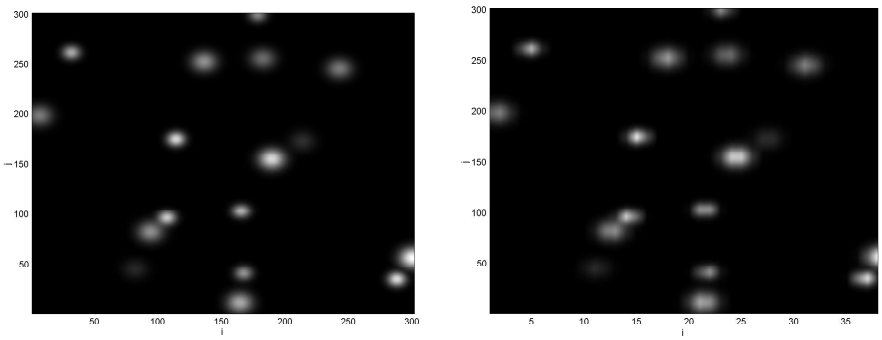

(a) High resolution image. (b) Low resolution image.

Fig. 2. Resolution decreasing with $c = H_{Res}^l / H_{Res} = 1/8$ along the i axis

From S^l, we obtain a set S^r (the superscript stands for "reconstructed") by means of an interpolation, in such a way that the images $I_k^r \in S^r$, $1 \leq k \leq N$ have the same resolution as $I_k \in S$. Let us denote $\hat{p}_k(i, j)$ the pixels of I_k^r obtained after the interpolation step. As performed in [8] in an OFDM context, we now propose a picture quality prediction in terms of PSNR, according to the

statistics of I_k, the factor c and the interpolation method. To this end, whatever $i = 1, .., V_{Res}$, we consider a pixel $\hat{p}_k\,(i,\, j_\delta)$ of I_k^r between two adjacent pixels $p_k\,(i,\, j_a)$ and $p_k\,(i,\, j_b)$. Given the resolution reduction, we have $j_b - j_a = 1/c$.

Since the images have a Gaussian intensity, we deduce from [8] that the interpolated images also have a Gaussian intensity. Consequently, the error $\xi = |p_k\,(i,\, j_\delta) - \hat{p}_k\,(i,\, j_\delta)\,|$ measured on an interpolated pixel follows a Chi distribution with one degree of freedom. For the NN interpolation, the error is noted ξ_{NN}, and is simply given by

$$\xi_{NN}(i, j_\delta) = |\sum_{m=0}^{M-1} \alpha_{m,k}\big(f_m\,(i,\, j_\delta) - f_m\,(i,\, j_a)\big)|, \tag{2}$$

for we have $\hat{p}_k\,(i,\, j_\delta) = p_k\,(i,\, j_a)$. For the linear interpolation, the error is noted ξ_{li}, and is derived from the Taylor's expansion of f_m on $(i,\, j_a)$ and $(i,\, j_b)$:

$$\xi_{li}(i, j_\delta) = \frac{1}{2}|(j_b - j_\delta)(j_a - j_\delta)| \times |p_k''\,(i,\, j_\delta)\,|, \tag{3}$$

where p_k'' is the second derivative of p_k, which is valid since the functions f_m are $\mathcal{C}^2$ on $\mathbb{R}^2$. Using the expression (1), we develop (3) to get:

$$\xi_{li}(i, j_\delta) = \frac{1}{2}|(j_b - j_\delta)(j_a - j_\delta)| \times |\sum_{m=0}^{M-1} \alpha_{m,k} f_m''\,(i,\, j_\delta)\,|. \tag{4}$$

From (2) and (4) and using the results of [8], we deduce the variance of the error $\sigma_\xi^2 = E\{\xi^2\}$, where $E\{.\}$ is the mathematical expectation. Bearing in mind that $\forall m = 0, .., M-1$, $\alpha_{m,k}$ are taken from independent zero-mean Gaussian processes, we obtain

$$\sigma_{\xi_{NN}}^2(i, j_\delta) = \sum_{m=0}^{M-1} \sigma_{\alpha_m}^2\big(f_m\,(i,\, j_\delta) - f_m\,(i,\, j_a)\big)^2, \tag{5}$$

$$\sigma_{\xi_{li}}^2(i, j_\delta) = \frac{1}{4}|(j_b - j_\delta)(j_a - j_\delta)|^2 \times \sum_{m=0}^{M-1} \sigma_{\alpha_m}^2 |f_m''\,(i,\, j_\delta)\,|^2. \tag{6}$$

The variances (5) and (6) define the local MSE on the pixels (i, j_δ). Let us define Δ the set of the coordinates j_δ corresponding to the interpolated pixels. Then, the total MSE, noted MSE_T is calculated by averaging on all the interpolated pixels as

$$MSE_T = \frac{1}{V_{Res}\, card(\Delta)} \sum_{i=1}^{V_{Res}} \sum_{j_\delta \in \Delta} \sigma_\xi^2(i, j_\delta), \tag{7}$$

with $card(\Delta)$ the cardinality of Δ. We finally deduce the PSNR:

$$PSNR = 10 \log_{10}\left(\frac{I_{max}^2}{MSE_T}\right), \tag{8}$$

where I_{max} is the maximum pixel value. From (5), (6), (7) and (8), we may state that the total MSE and the PSNR depends on the factor c (or equivalently on the size of Δ), the functions f_m and the second-moment order of the image σ_m^2. Since all these parameters are known, the quality characteristics MSE_T and $PSNR$ are deterministic and can be a priori estimated, which is verified in the next section.

4 Simulations Results

4.1 Simulations Parameters

In order to validate the previous developments, we use the two sets *stars* and *waves*, each composed of 2600 images. The resolutions of the pictures of *stars* and *waves* are $V_{Res} = H_{Res} = 301$ and $V_{Res} = H_{Res} = 401$ pixels, respectively. Table 1 gives the positions of the centers of the 18 stars that compose the images in *stars*, and the variance of their intensity is given in the third row. For *waves*, Table 2 gives the directions and the variance of the 10 waves that compose the images. In our simulations, the pixels are represented using 8 bits, so I_{max}=255.

Table 1. Table of parameters for the stars images.

i axis	45	16	297	56	234	144	87	166	10	286	33	226	262	90	238	277	132	189
j axis	228	167	179	293	211	280	68	52	107	227	86	280	282	254	137	255	86	260
σ_{α_m}	0.8	0.64	0.18	0.53	0.22	0.55	0.06	0.59	0.42	0.19	0.06	0.07	0.31	0.94	0.98	0.56	0.99	0.69

Table 2. Table of parameters for the waves images.

c_{mx}	-0.58	0.66	-0.36	-0.41	0.86	-0.23	0.62	0.59	0.91	0.97
c_{my}	-0.16	0.72	0.64	-0.84	-0.67	-0.03	-0.19	-0.96	0.71	-0.5
σ_{α_m}	0.8	0.64	0.18	0.53	0.22	0.55	0.06	0.59	0.42	0.19

4.2 MSE and PSNR of the Interpolated Images

The tables 3 and 4 present the results obtained for the *stars* and *waves* sets. In these tables, $D_{max}(X)$ represents the maximum value of the absolute difference between the a posteriori measurement X^S , and the a priori measurement X^A, that is $D_{max}(MSE) = \max_{i,j_\delta} \left(\left| \sigma_(i, j_\delta)^S - \sigma_(i, j_\delta)^A \right| \right)$, with $\sigma_(i, j_\delta)^A$ defined as in (5) or (6), $D(MSE_T) = \left(\left| MSE_T^S - MSE_T^A \right| \right)$, with MSE_T^A defined as in (7) and $D(PSNR) = \left(\left| PSNR^S - PSNR^A \right| \right)$, with $PSNR^A$ defined as in (8).

The measurements $D_{max}(MSE)$ are presented so as to give an idea of local maxima of the difference between a priori and a posteriori calculations. Indeed, as large part of the images belonging to this set consist only on a uniform background (namely for the *stars* set), interpolating pixels there will not lead to any error, as depicted in Fig. 3, thus diminishing the mean value $D(MSE_T)$.

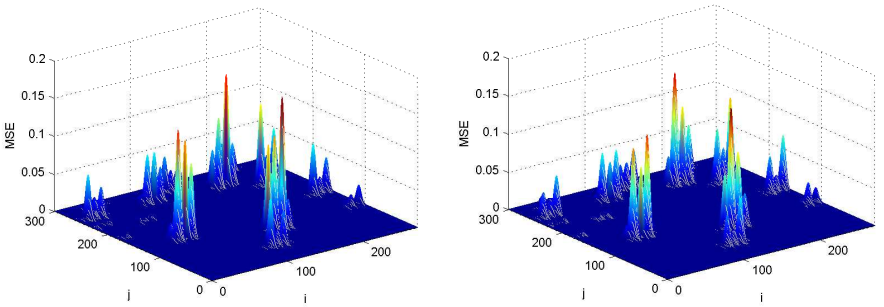

(a) Simulation. (b) Analysis.

Fig. 3. MSE versus (i, j) of NN-interpolated images from *stars* with $c = 10$.

Table 3. Measures for *stars*

stars	NN			linear		
c	2	4	10	2	4	10
$D_{max}(MSE)$	2.9×10^{-3}	1.31×10^{-2}	1.45×10^{-1}	8.97×10^{-6}	2.79×10^{-4}	1.75×10^{-2}
$D(MSE_T)$	2.62×10^{-5}	6.21×10^{-5}	3.11×10^{-4}	4.84×10^{-8}	1.34×10^{-6}	9.57×10^{-5}
$D(PSNR)$ in dB	-0.12	0.06	-0.17	0.09	0.31	0.86
$PSNR$ ref in dB	81.9	79.09	72.25	103.34	93.02	78.35

The disparity between $D_{max}(MSE)$ and $D(MSE_T)$ is not as significant for the *waves* set as for the *stars* set, because wave images are built from sums of continuous cosine contributions, and interpolations therefore produce errors everywhere on the image.

The values we obtained are consistent: one can observe the PSNR we estimate follows the trend of the a posteriori calculated PSNR, decreasing when the column suppression factor c increases. Besides, the estimated values are very close to the measured ones. We also notice the results obtained for linear interpolation are significantly better than those obtained for the NN-interpolation. This can be easily explained by the better precision of the linear interpolation compared to the NN one. Consequently, we verify that the proposed method allows a very accurate error estimation.

4.3 Discussion and Further Works

The method yields very good results on highly synthetic images, and with simple low order interpolation techniques. With regards to such results, the proposed analysis may lead to consider practical implementations. For instance, an obvious application is to use the technique for image quality prediction. In order to extend that, the quality prediction may enable an adaptive resolution process, in function of a target image quality that can be a priori accurately computed. We plan to further investigate our method with the following objectives in mind:

- tests with higher order interpolations, such as spline or bicubic interpolator,
- extension of the analysis whatever the image probability density,
- modification of the resolution along both dimensions,
- tests on real images.

We shall have two different image types for our tests on real image sets. First, we shall test the method on images which resemble the highly synthetic test images we first used, that is photos of starred skies, of sea clutter and waves, of cloud formations, or any real image which we could reasonably approximate with sums of Gaussian distributions. On the other hand, we shall test images with no assumption about their Gaussian nature whatsoever. If need be, we shall also test the method locally in these images, selecting areas for which theoretical requirements are met, or for which the Gaussian assumption holds true. As aforementioned, this latter consideration opens another exciting perspective: one could imagine choosing different interpolations techniques given a region within the image, thus designing an adaptive interpolation system.

Table 4. Measures for *waves*

waves	NN			linear		
c	2	4	10	2	4	10
$D_{max}(MSE)$	5.46×10^{-4}	1.8×10^{-3}	2.47×10^{-2}	2.2×10^{-7}	3.35×10^{-6}	1.42×10^{-4}
$D(MSE_T)$	1.41×10^{-4}	2.23×10^{-4}	1.7×10^{-3}	6.59×10^{-8}	6.52×10^{-7}	2.72×10^{-5}
$D(PSNR)$ in dB	9.15×10^{-2}	-0.11	0.145	0.2	-0.04	-0.25
$PSNR$ ref in dB	70.26	67.05	60.57	103.67	92.9	77.54

5 Conclusion

This paper dealt with a method for the a priori picture quality measurement in image processing. Interpolations are usually required when decompressing images or when reconstructing damaged images, inducing errors that deteriorate the picture quality. In the literature, some common quality measurements such as the MSE or the PSNR a posteriori characterize the interpolated image quality. We here proposed to a priori perform this measurements, using the statistical properties of the images, and we showed the accuracy of our method, in comparison to the a posteriori measurements. Thus, for an expected picture quality, the proposed analysis allows to a priori choose the resolution decreasing factor c and the interpolation method that fulfill the better trade-off between data rate and complexity. The developments was achieved considering the simple NN and the linear interpolation, but we are investigating the analysis with higher-order interpolator functions. Moreover, a resolution decreasing over the two dimensions has to be considered, and a practical implementation on more realistic pictures would be interesting for a practical implementation.

References

1. Mrak, M., Grgic, S., Grgic, M.: Picture quality measures in image compression systems. In: EUROCON 2003, Ljubljana, Slovenia, vol. 1, pp. 233–236 (2003)
2. Scharinger, J.: Image compression by multilevel polynomial interpolation and wavelet texture coding. In: Moreno-Díaz, R., Pichler, F. (eds.) EUROCAST 1997. LNCS, vol. 1333, pp. 429–443. Springer, Heidelberg (1997)
3. Maaß, P., Stark, H.G.: Wavelets and Digital Image Processing (1994)
4. Lehmann, T.M., Gönner, C., Spitzer, K.: Survey: Interpolation Methods in Medical Image Processing. IEEE Transactions on Medical Imaging 18(11), 1049–1075 (1999)
5. Titus, J., Geroge, S.: A Comparison Study On Different Interpolation Methods Based On Satellite Images. International Journal of Engineering Research & Technology 2(6), 82–85 (2013)
6. Dhingra, R., Singh, S.: Comparison of Various Interpolation Based Image Zooming Techniques. International Journal of Advanced Research in Computer Science and Software Engineering 3(6), 1580–1583 (2013)
7. Han, D.: Comparison of Commonly Used Image Interpolation Methods. In: ICCSEE, Hangzhou, China (2013)
8. Savaux, V.: Contributions l'estimation de canal mutli-trajets dans un contexte de modulation OFDM - Contribution to multipath channel estimation in a context of OFDM modulation. PhD thesis, Supélec, Rennes, France (2013)